

# Nanoscale

Accepted Manuscript



This is an *Accepted Manuscript*, which has been through the Royal Society of Chemistry peer review process and has been accepted for publication.

*Accepted Manuscripts* are published online shortly after acceptance, before technical editing, formatting and proof reading. Using this free service, authors can make their results available to the community, in citable form, before we publish the edited article. We will replace this *Accepted Manuscript* with the edited and formatted *Advance Article* as soon as it is available.

You can find more information about *Accepted Manuscripts* in the [Information for Authors](#).

Please note that technical editing may introduce minor changes to the text and/or graphics, which may alter content. The journal's standard [Terms & Conditions](#) and the [Ethical guidelines](#) still apply. In no event shall the Royal Society of Chemistry be held responsible for any errors or omissions in this *Accepted Manuscript* or any consequences arising from the use of any information it contains.



## Unexpected electronic perturbation effects of simple PEG environments on the optical properties of small cadmium chalcogenide clusters†

Received 00th January 20xx,  
Accepted 00th January 20xx

DOI: 10.1039/x0xx00000x

www.rsc.org/

Naoto Fukunaga<sup>a</sup> and Katsuaki Konishi<sup>\*ab</sup>

Poly(ethylene glycol) (PEG) has been widely used for the surface protection of inorganic nanoobjects because of its virtually 'inert' nature, but less attention has been paid to its inherent electronic impacts on inorganic cores. Herein, we definitively show, through studies on optical properties of a series of PEG-modified Cd<sub>10</sub>Se<sub>4</sub>(SR)<sub>10</sub> clusters, that surrounding PEG environments can electronically affect the properties of the inorganic core. For the clusters with PEG units directly attached to an inorganic core (R = (CH<sub>2</sub>CH<sub>2</sub>O)<sub>n</sub>OCH<sub>3</sub>, PEG<sub>n</sub>, n = 3, ~7, ~17, ~46), the absorption bands, associated with the low-energy transitions, continuously blue-shifted with increasing PEG chain length. The chain length dependencies were also observed in the photoluminescence properties, particularly in the excitation spectral profiles. By combining the spectroscopic features of several PEG17-modified clusters (**2**-C<sub>m</sub>-PEG17 and **3**) whose PEG and core units are separated by various alkyl chain-based spacers, it was demonstrated that sufficiently long PEG units, including PEG17 and PEG46, cause electronic perturbations in the cluster properties when they are arranged near the inorganic core. These unique effects of the long-PEG environments could be correlated with their large dipole moments, suggesting that the polarity of the proximal chemical environment is critical when affecting the electronic properties of the inorganic cluster core.

### Introduction

Nanoparticle/cluster compounds protected by organic ligands continue to receive interest because of their unique electronic, optical and catalytic properties.<sup>1</sup> Conventional colloidal nanoclusters with inorganic core sizes of several nanometres or above have been extensively studied, and it is well established that their properties are dependent on the size (nuclearity), generally referred to as quantum effects.<sup>2–4</sup> However, when the size of the inorganic core is decreased to approximately 2 nm, molecule-like behaviours due to discrete electronic structures emerge instead. In such a size regime, the electronic properties should not only be affected by the core nuclearity but also by the core microstructure and surface organic ligands. Recent progress in the crystallographic characterisation of very small cluster compounds has revealed that core structures critically affect their electronic/optical features.<sup>5–8</sup> On the other hand, the effects of surrounding organic environments remain elusive.

Certain organic ligands have been reported to electronically interact (couple) with the inorganic core of semiconductor quantum dots through coordination bonds, causing substantial alterations to the optical spectra.<sup>9–13</sup> In addition to these electronic perturbations associated with local coordination events, the steric/electronic character of the organic moiety as an encapsulating environment should affect the electronic properties of the inorganic core, but these aspects have rarely been studied to date.<sup>14</sup> Molecular-sized clusters would offer suitable models to investigate the possible effects of the organic environment since most of the atoms constituting the inorganic core are located on the surface.

Poly(ethylene glycol) (PEG), also known as poly(ethylene oxide) (PEO), has been widely used for the stabilisation of metal-containing cluster compounds, particularly for biomedical/ biochemical purposes, because of their high water solubility and biocompatibility.<sup>15–18</sup> The surrounding PEG chains sterically protect and insulate the inorganic core from the outer environment, but the impact of the PEG units, on the properties of the cluster core, has not been clarified. We previously explored guest-sensing functions in aqueous media using luminescent PEG-modified CdS-based clusters with the general formula, Cd<sub>10</sub>S<sub>4</sub>(SR)<sub>12</sub>.<sup>19,20</sup> Over the course of this study we noticed that their UV absorption profiles, which virtually reflect the electronic properties of the inorganic core units, unexpectedly varied with the surface organic units. This

<sup>a</sup> Graduate School of Environmental Science, Hokkaido University, North 10 West 5, Sapporo 060-0810 Japan.

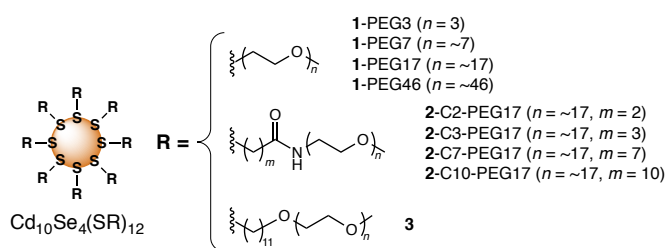
E-mail: konishi@ees.hokudai.ac.jp; Fax: +81 11 7064538; Tel: +81 11 7064538

<sup>b</sup> Faculty of Environmental Earth Science, Hokkaido University, North 10 West 5, Sapporo 060-0810 Japan.

† Electronic Supplementary Information (ESI) available: Details of synthetic procedures and characterisation data of the PEGylated thiols and clusters and additional absorption, photoluminescence emission and excitation spectra data. DOI: 10.1039/x0xx00000x

observation motivated us to further investigate the nature of the PEG effects on the optical properties of the inner inorganic core.

In the present paper, we employed  $\text{Cd}_{10}\text{Se}_4(\text{SR})_{12}$ -type clusters with various PEG-containing organic units (**1–3**) and systematically studied their optical absorption and photoluminescence properties in terms of the PEG chain length and PEG-to-core distance. Here, we used  $\text{Cd}_{10}\text{Se}_4(\text{SR})_{12}$  rather than  $\text{Cd}_{10}\text{S}_4(\text{SR})_{12}$  because the latter exhibits cluster absorptions below 350 nm, which are mostly overlapped with the ligand-originated transitions. By studying the optical spectral features of **1**, with PEG units of various lengths directly attached to the core, we definitively show that simple PEG moieties can affect the electronic structure of the inorganic core. By combining the spectral features of the clusters bearing PEG units separated from the core by appropriate spacers, we discuss the nature of electronic perturbation effects of the PEG units on the electronic properties of the cluster. Although the optical spectra dependency on the PEG chain length has recently been reported in some colloiddally synthesised CdSe clusters,<sup>21</sup> the present approach, using molecular clusters, is advantageous since the core units are essentially identical to each other, excluding the possible contribution of the subtle differences in the inorganic core units.



## Experimental Section

### General

$^1\text{H-NMR}$  spectra were recorded in  $\text{CDCl}_3$  on JEOL ECX400 (400 MHz) at room temperature. The chemical shifts of  $^1\text{H-NMR}$  spectra were determined with a solvent signal ( $\text{CHCl}_3$ : 7.26 ppm). MALDI-TOF-MS spectra were recorded on SHIMADZU AXIMA-CFR with the linear mode and 2,5-dihydroxybenzoic acid as a matrix. FT-IR spectra were recorded in KBr pellets on a JASCO Type FT/IR-400. ATR-IR spectra in water were recorded by JASCO Corporation with a JASCO FT/IR-4600 coupled with a JASCO ATR PRO 450-S module, and the background absorption of water was subtracted from the raw spectral data. UV-Vis absorption spectra were recorded on a JASCO V-550 UV/VIS spectrometer with peak resolution of 0.2 nm using a quartz cell with a 1-cm path length. Photoluminescence emission and excitation spectra were recorded with peak resolution of 1.0 nm on a JASCO FP-6500 spectrofluorometer equipped with a Hamamatsu Photonics R928 photomultiplier tube detector, and corrected by using rhodamine B and a JASCO ESC-333 standard light source unit. An optical filter was applied before the detector window to remove wavelengths below 360 nm, thus avoiding the second-

order effects of the excitation light. Thermogravimetric analysis (TGA) profiles were obtained on a Rigaku thermo plus TG 8120 in a temperature range between room temperature and 475 °C with scan rate of 2 °C/min under air flow of 100 ml/min.

### Materials

Poly(ethylene glycol) monomethyl ether ( $\text{HO}(\text{CH}_2\text{CH}_2\text{O})_n\text{CH}_3$ ,  $M_w = 350$ ) was purchased from Alfa Aesar. Poly(ethylene glycol) monomethyl ether ( $\text{HO}(\text{CH}_2\text{CH}_2\text{O})_n\text{CH}_3$ ,  $M_w = 750$  and 2000) were purchased from Aldrich. The averaged degrees of polymerization ( $n$ ) of the poly(ethylene glycol) monomethyl ethers were checked by MALDI-MS measurements and estimated to be  $\sim 7$  ( $M_w = 350$ ),  $\sim 17$  ( $M_w = 750$ ) and  $\sim 46$  ( $M_w = 2000$ ). Tri(ethylene glycol) monomethyl ether, potassium phthalimide (>98%), 3,3'-dithiodipropionic acid (>99%), 1-ethyl-3-(3-dimethylaminopropyl)carbodiimide hydrochloride (>98%) and benzenethiol (>98%) were purchased from TCI. Toluenesulfonyl chloride (>97%), thiourea (>98%), methylamine (40%, aqueous solution), sodium borohydride (>90%), cadmium nitrate tetrahydrate (>98%), tetraethylammonium chloride (>98%) and selenium powder (>99%) were purchased from Wako Chemical. 4,4'-Dithiodibutyric acid (>95%), 8-mercaptooctanoic acid (>95%) and 11-mercaptoundecanoic acid (>95%) were purchased from Aldrich. Triethylamine (>99%) and sodium hydroxide (>97%) were purchased from Nacalai Tesque. 1-Hydroxybenzotriazole (>99%) was purchased from Dojindo. Other standard chemicals and solvents were obtained from Wako Chemical or Kant Chemical or Nacalai Tesque. The reagents and solvents were used as received without further purification.  $[\text{Cd}_{10}\text{Se}_4(\text{SPh})_{12}](\text{NMe})_4$  was synthesised from  $[\text{Cd}_4(\text{SPh})_{10}](\text{NMe})_2$  and element selenium according to the literatures.<sup>22</sup>  $\text{Cd}_{10}\text{Se}_4(\text{SPh})_{12}$  was prepared from  $[\text{Cd}_{10}\text{Se}_4(\text{SPh})_{12}](\text{NMe})_4$  using a modified literature procedure.<sup>23,24</sup> In the literature,<sup>24</sup>  $\text{Cd}_{10}\text{Se}_4(\text{SPh})_{12}$  was synthesized by pyrolysis of  $[\text{Cd}_{10}\text{Se}_4(\text{SPh})_{12}](\text{NMe})_4$  under vacuum at 300 °C for 15 min. We found that the same compound was obtained upon heated under vacuum at 160 °C for 8 h. After the heat treatment, the resulting yellow residue was washed with hexane and chloroform, and dried under vacuum. Calcd (%) for  $\text{Cd}_{10}\text{Se}_4\text{S}_{12}(\text{C}_6\text{H}_5)_{12}$ : C 31.45, H 2.20, N 0, S 13.99; found: C 31.15, H, 2.25, N, 0, S, 13.97.

### Syntheses of PEGylated thiols and clusters

Thiol-terminated PEGs ( $\text{HS-PEG}_n$ ) for the syntheses of **1-PEG<sub>n</sub>** were prepared from tri(ethylene glycol) monomethyl ether ( $n = 3$ ) and poly(ethylene glycol) monomethyl ethers ( $n = \sim 7, \sim 17$  and  $\sim 46$  for  $M_w = 350, 750$  and 2000, respectively) by standard organic synthesis methods.  $\text{HS}-(\text{CH}_2)_m\text{-CONH-PEG17}$  for the syntheses of **2-C<sub>m</sub>-PEG17** ( $m = 2, 3, 7, 10$ ) were prepared from amino-terminated poly(ethylene glycol) monomethyl ethers with  $M_w$  of 750. The outline of the synthetic schemes and detailed procedures were given in Electronic supporting information.

General synthesis of PEGylated clusters: To a glass vial containing  $\text{Cd}_{10}\text{Se}_4(\text{SPh})_{12}$  (132.9 mg, 48.3  $\mu\text{mol}$ ) and

PEGylated thiol (5.80 mmol) were added distilled water (10 ml) and methanol (1 ml), and the mixture was stirred at room temperature. The initial suspension became homogeneous gradually to give a yellow solution. After 1 h, ether (20 ml) was added into the reaction solution, and then the two-layered reaction mixture was stirred for additional 24 h at room temperature under dark. After the separated ether layer containing thiophenol was discarded, the aqueous layer collected was subjected to repeated dialysis against Milli-Q deionised water using Biotech Spectra/Por® (RC, MWCO = 3500) to remove unreacted thiols. The aqueous solution was freeze-dried to give a pale yellow tan solid. The yields were almost quantitative. The complete exchange of the thiolate ligands was checked by FT-IR (KBr pellet) (Fig. S1) and  $^1\text{H}$  NMR spectra ( $\text{CDCl}_3$ ) (Fig. S2), which showed no IR vibration bands and NMR signals due to the residual phenyl group. The PEGylated clusters were further analyzed by TGA. Upon heated to 450 °C under air, the parent phenyl-capped cluster  $\text{Cd}_{10}\text{Se}_4(\text{SPh})_{12}$  showed a weight decrease of 34.5%, which matched well with the mass fraction of the organic (phenyl) moieties (33.6%), indicating that the surface organic moieties were lost during the heating process. Likewise, the observed weight losses of the PEGylated clusters almost agreed with the calculated mass fraction of the organic units of  $\text{Cd}_{10}\text{Se}_4(\text{SR})_{12}$  (Fig. S3 and Table S1), supporting the simple ligand exchange with retention of the ' $\text{Cd}_{10}\text{Se}_4\text{S}_{12}$ ' core.

### Spectral Measurements

The samples for absorption and photoluminescence spectral measurements were prepared by diluting concentrated cluster solutions with an absorbance of approximately 0.1 at 390 nm. The concentrations could not be correctly determined because of the hygroscopic nature of the PEG-modified clusters but were estimated to be approximately 15  $\mu\text{M}$ .

## Results

### Synthesis of PEGylated clusters.

In previous papers, we reported that the phenyl-capped  $\text{Cd}_{10}\text{S}_4(\text{SPh})_{12}$  reaction with thiols (RSH) results in a simple thiolate exchange and  $\text{Cd}_{10}\text{S}_4$  core retention to give  $\text{Cd}_{10}\text{S}_4(\text{SR})_{12}$ .<sup>19,20,25,26</sup> Similarly, a series of PEG-functionalised  $\text{Cd}_{10}\text{Se}_4(\text{SR})_{12}$  clusters (**1–3**) were prepared by the thiolate exchange reaction of  $\text{Cd}_{10}\text{Se}_4(\text{SPh})_{12}$ <sup>24</sup> with PEGylated thiols. Triethylene glycol monomethyl ether (PEG3) and poly(ethylene glycol) monomethyl ethers, with number average molecular weights of 350, 750 and 2000 (i.e. PEG7, PEG17 and PEG46, respectively), were used as precursors for the PEGylated thiols. The ligand exchange reactions were first conducted in water/methanol and then switched to the biphasic system by ether addition, which simplified the separation of the PEG-modified cluster formations in the aqueous phase by extracting the liberated thiophenol into the organic phase. IR spectra of the ligand-exchanged products show no vibrational absorptions owing to the surface phenyl groups of  $\text{Cd}_{10}\text{Se}_4(\text{SPh})_{12}$  but clearly show new bands as a result of the PEG moieties (Fig.

S1). Consistently,  $^1\text{H}$  NMR spectra show no signals because of the residual phenyl groups (Fig. S2). Thus,  $\text{Cd}_{10}\text{S}_4(\text{SPh})_{12}$  surface phenyl groups were completely exchanged with organic units containing PEG.

### Optical properties of directly PEGylated clusters (**1**).

In contrast to the parent phenyl-capped cluster  $\text{Cd}_{10}\text{Se}_4(\text{SPh})_{12}$ , the PEG-modified clusters (**1–3**) exhibit high water solubility. The optical absorption spectra of **1–3** measured in Milli-Q water (pH = ~7) at 20 °C showed three apparent bands between 300–500 nm. For example, **1-PEG3** show bands at 387.2, 357.8 and 335.8 nm (Fig. 1 and Table 1, entry 1). Since these bands are considered to result from the optical transitions from Se (4p) or S (3p) to Cd (5s) orbitals,<sup>27</sup> one would expect the same absorption spectra for the other clusters having long PEGchains if the inorganic core is electronically intact. However, as shown in Figs. 1 and 2, definite blue shifts were observed when the PEG chain length was increased. The shift of the second band ( $\lambda_2$ ) was especially remarkable. A blue shift of 16.8 nm (357.8  $\rightarrow$  341.0 nm) was observed when the surface PEG3 units of **1-PEG3** were swapped with the longer PEG7 units (Fig. 1 and Table 1, entry 4). A comparably large shift was observed for the third band (335.8  $\rightarrow$  316.0 (shoulder) nm).

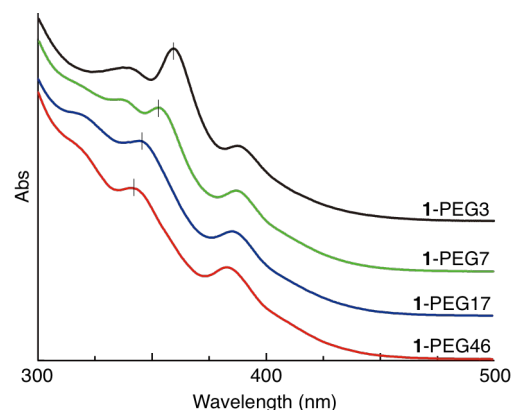


Fig. 1 Absorption spectra of **1-PEG3**, **1-PEG7**, **1-PEG17** and **1-PEG46** in deionized water at 20 °C. Ticks represent the second absorption bands ( $\lambda_2$ ).

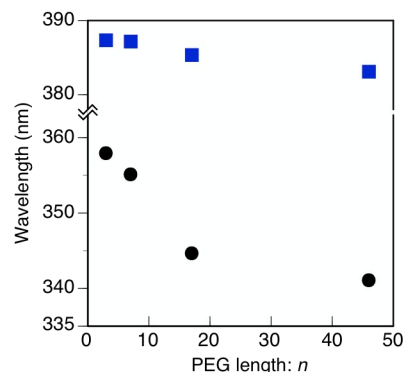


Fig. 2 Plots of the absorption band positions ( $\lambda_1$  (■),  $\lambda_2$  (●)) of **1-PEG<sub>n</sub>** ( $n = 3, 7, 17$  and  $46$ ) versus PEG-chain length ( $n$ ) in deionized water at 20 °C.

**Table 1** Electronic absorption, photoluminescence emission (PL) and photoluminescence excitation (PLE) spectral data of PEG-modified Cd<sub>10</sub>Se<sub>4</sub>(SR)<sub>12</sub> clusters in deionized water at 20 °C.

entry	cluster	Abs		PL <sup>a</sup>	PLE <sup>b,c</sup>
		$\lambda_1$ /nm	$\lambda_2$ /nm	$\lambda_{em}$ /nm	$\lambda$ /nm
1	1-PEG3	387.2	357.8	605	372(s), 393
2	1-PEG7	387.0	355.0	601	371(s), 387, 411(s)
3	1-PEG17	385.2	344.5	596	367(s), 387, 407(s)
4	1-PEG46	383.0	341.0	590	363(s), 387, 404(s)
5	2-C2-PEG17	383.0	341.0	588	361(s), 387, 404(s)
6	2-C3-PEG17	385.8	348.0	592	367(s), 387, 406(s)
7	2-C7-PEG17	387.4	355.6	592	370(s), 393
8	2-C10-PEG17	389.6	355.6	594	371(s), 393
9	3	389.4	355.8	582	372(s), 393

$\lambda_{ex}$  = 393 nm. <sup>b</sup> monitored at 580 nm. <sup>c</sup> (s): shoulder band.

whereas the shift of the first band was much smaller (387.2 → 383.0 nm). Considering that the PEG chains are linked to the S atoms, the second and third bands are likely due to the S-mediated transitions because they were affected more by the PEG units than the first band. Accordingly, the transitions associated with the first band are considered to involve Se atoms. The plots of the wavelength positions of the first ( $\lambda_1$ ) and second bands ( $\lambda_2$ ) versus the PEG chain length ( $n$ ) (Fig. 2) show that the blue shifts almost reached saturation at  $n$  = approximately 50.

The PEG chain length dependency was also observed in the photoluminescence profiles. Similar to the Cd<sub>10</sub>S<sub>4</sub>(SR)<sub>12</sub> clusters,<sup>19,20,25,26</sup> upon excitation of the cluster moiety at 393 nm, **1** exhibits a broad photoluminescence emission (PL) band at approximately 600 nm, which may be associated with the

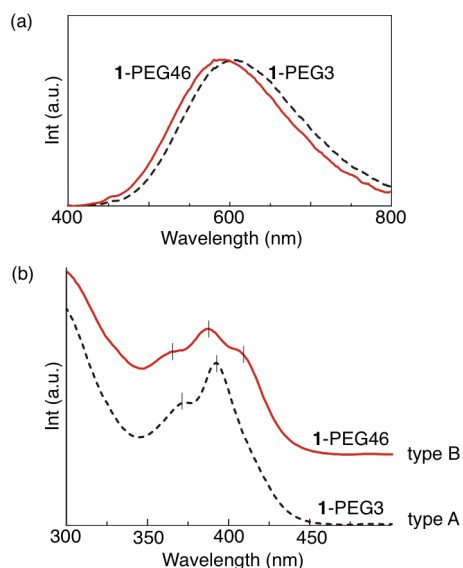


Fig. 3 Corrected photoluminescence emission (PL,  $\lambda_{ex}$  = 393 nm) (a) and excitation (PLE, monitored at 580 nm) (b) spectra of **1**-PEG3 (dashed) and **1**-PEG46 (solid) in deionized water at 20 °C.

surface-induced radiation process (trap emission). With the increase of the PEG chain length, the emission band slightly blue shifted (Table 1, entries 1–4 and Fig. S4) along with bandwidth retention. For example, the emission band of **1**-PEG3 was observed at 605 nm, whereas **1**-PEG46 gave a band at 590 nm (Fig. 3a). On the other hand, a more explicit change with the increase of the PEG chain length was observed in the photoluminescence excitation (PLE) spectra. As shown in Fig. 3b, **1**-PEG3, with the shortest PEG chains, gave a bimodal profile with a band at 393 nm, together with a shoulder band at approximately 370 nm when monitored at 580 nm. Upon increasing the PEG chain length, these two bands slightly shifted towards blue wavelengths and a new shoulder band developed at approximately 410 nm (Fig. S5a) to give a trimodal pattern, as seen in the spectrum of **1**-PEG46 (Fig. 3b). It should be noted that the PLE spectra did not coincide with the absorption spectra. For example, in the excitation spectra of **1**-PEG46, the main band at 387 nm could be correlated to the first absorption band, but no apparent bands/shoulders were observed at approximately 370 and 410 nm in the absorption spectrum (Fig. 1). Therefore, the clusters intrinsically have several excitation transitions with PL-active and PL-inactive characters, some of which are, however, obscured in the absorption spectra.

#### Effects of the PEG-to-core distance

The above results suggest that the PEG units attached to the inorganic core can greatly affect the cluster optical transitions and electronic structures. For further insight, we subsequently investigated the effective distance between the PEG and the inorganic core for the PEG17-modified family. Alkylamide spacers  $-(CH_2)_mCONH-$  with linear various alkyl chain lengths (**2**,  $m$  = 2, 3, 7, 10) were inserted between the core and the PEG units. As shown in Fig. 4, the cluster absorption bands nearly coincided with those of the non-spacer type analogue (**1**-PEG17, entry 3). However, upon increasing the spacer lengths, the bands were red-shifted to reach the **1**-PEG3 positions (Figs. 5 and S6). For instance, the first and second bands of **2**-C10-PEG17 appeared at nearly identical positions compared with those of **1**-PEG3 and exhibited similar spectral patterns (Fig. 4). The third band was overlapped with the band at ~320 nm but found as a minor shoulder at ~340 nm.† The amide groups in the spacer units of **2** appeared to have little contribution to this spectral change, since **3**, with simple  $-(CH_2)_{11}$ -PEG17 substituents, also exhibited similar spectral patterns and band positions to **1**-PEG3 (Table 1, entry 9 and Fig. S7).

The effect of spacer length on the optical features was also observed in the PLE profiles. **2**-C2-PEG17 and **2**-C3-PEG17 with short spacers, exhibit three bands (Fig. S5b) and show similar spectral patterns to that observed for **1**-PEG17 (Fig. S5a) (Table 1). On the other hand, the spectral profiles of **2**-C7-PEG17, **2**-C10-PEG17 and **3**, whose PEG17 units are spatially separated from the inorganic core, were clearly different and exhibit bimodal patterns (Fig. S5b), which were quite similar to that of **1**-PEG3 (Fig. 3b). Accordingly, the general trend in the

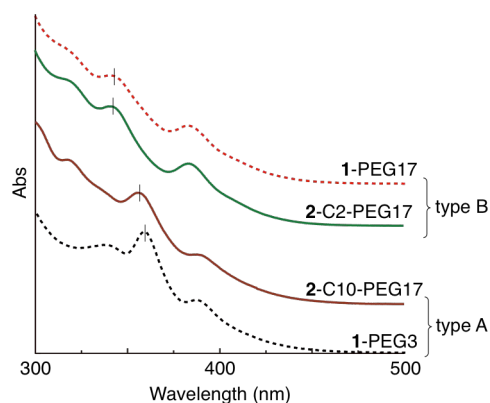


Fig. 4 Absorption spectra of **1-PEG3**, **2-C10-PEG17**, **2-C2-PEG17**, and **1-PEG17** in water at 20 °C.

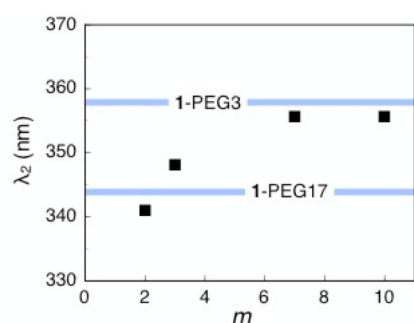


Fig. 5 Plot of the position of the second absorption band ( $\lambda_2$ ) of **2-Cm-PEG17** versus  $m$  in water at 20 °C. Blue lines represent the positions of the second absorption bands of **1-PEG3** and **1-PEG17**.

PLE spectral profiles matched well with that of the absorption spectral profiles. Thus, the clusters with PEG17 units located near the inorganic core, such as **1-PEG17**, **2-C2-PEG17** and **2-C3-PEG17**, have essentially similar electronic structures to each other. However, they varied as the PEG-to-core distance increased (as in **2-C7-PEG17** and **2-C10-PEG17**) and exhibit spectral profiles close to that of **1-PEG3** with short PEG chains. On the other hand, such clear trends were not observed in the emission spectra (Fig. S4b), suggesting that the governing factor responsible for the radiative process is virtually different from the excitation processes.

## Discussion

As we have seen, the optical properties of the PEG-modified clusters (**1–3**) vary substantially with PEG length or PEG-to-core distance. Since the surface organic groups used in this study have negligible absorptions above 300 nm, the electronic coupling of the organic moieties with the inorganic core appears unlikely. Thus, their absorption and PLE spectral features should virtually reflect the electronic structure of the inorganic core. Considering all of the spectral data, the present  $\text{Cd}_{10}\text{Se}_4(\text{SR})_{12}$  clusters intrinsically have two types of absorption/PLE spectral patterns, and hence, the clusters are

categorised into two groups in terms of the spectral features (Fig. 6). One group constitutes **1-PEG3**, **2-C7-PEG17**, **2-C10-PEG17** and **3** which exhibit absorption spectra with the second band ( $\lambda_2$ ) at a higher wavelength ( $\sim 357$  nm) and two-band PLE spectra (type A, Figs. 3b and 4). Alternatively, **1-PEG17**, **1-PEG46** and **2-C2-PEG17** exhibit a blue-shifted second absorption band ( $\lambda_2 =$  approximately 341 nm) and three-band PLE spectrum (type B). The spectra of **1-PEG7** and **2-C3-PEG17** lie at intermediates between the types A and B, which can be described as the combination of two spectral patterns (Figs. 1 and S5).

type A	type B
<b>1-PEG3</b>	<b>1-PEG17</b>
<b>2-C7-PEG17</b>	<b>1-PEG46</b>
<b>2-C10-PEG17</b>	<b>2-C2-PEG17</b>
<b>3</b>	
Abs: $\lambda_2 = \sim 357$ nm	Abs: $\lambda_2 = \sim 341$ nm
PLE: two bands	PLE: three bands

Fig. 6 Categorisation of the clusters in terms of the absorption and PLE spectral patterns

Among the series of directly attached PEGylated clusters (**1-PEG $n$** ), **1-PEG3** exhibits the least steric hindrance in the surface environment. Therefore, its optical properties may be altered through coordinative interactions of water molecules in the inorganic surface. However, such a possibility is unlikely since the absorption spectrum in coordinative inert solvents, e.g. dichloromethane, was nearly identical to that in water (Fig. S8). Thus, the type A absorption and PLE spectra observed for **1-PEG3** are considered reflective of the electronic properties of intact cluster species, whereas type B spectra of **1-PEG17** and **1-PEG46** may arise from the electronic effects of long PEG chains. As found from the PEG-to-core distance effects from the PEG17-modified family, the clusters with short alkyl chain spacers (**2-C2-PEG17**, **2-C3-PEG17**) exhibit type B spectra, but as the spacer length increases (**2-C7-PEG17**, **2-C10-PEG17**), the spectral pattern approaches type A observed for **1-PEG3** (Figs 4, 5 and S6). This observation implies that the PEG17 shell can cause effective perturbations to the cluster electronic structures when they are in proximity of the core. This effect is only minor when spatially separated. Thus, not only is the chain length a critical factor affecting the perturbation effects of long PEG units but also the distance from the inorganic core.

The unique capability of the long PEG units to affect the optical properties of the proximal inorganic core, as observed in **1-PEG17** and **1-PEG46**, is interesting considering that PEG is generally considered to be essentially inert. The introduction of long PEG chains to the inorganic surface may result in effective core coverage by the PEG chains. However, such a factor does not appear responsible for the observed PEG chain length dependency, since the clusters with sufficiently hindered surface environments (e.g. **2-C10-PEG17**) exhibited type-A absorption and PLE spectra, which are different from the type-B spectra of **1-PEG17** and **1-PEG46** (Figs. 4, 6 and S5).

On the other hand, the dipole moment of the linear PEG chain is known to increase with the chain length.<sup>28,29</sup> This trend

has been explained to result from conformational isomerism about the single bonds of the individual ethylene glycol units.<sup>30–34</sup> The *trans* (anti)–gauche conformational arrangement about the C–C bond has an especially profound effect; the gauche conformation generates a larger dipole moment than that of the *trans* conformation,<sup>35</sup> so the large dipole moment of long PEG can be correlated to the enhanced gauche content in the polymer chains. In order to check that the PEGs on the clusters also have such chain-length-dependent conformational characters, we conducted IR analyses. According to the previous literatures concerning the IR spectroscopic studies of free PEGs,<sup>33,36</sup> the CH<sub>2</sub> wagging/twisting vibrations of the gauche and *trans* conformers are observed at ~1350 and ~1325 cm<sup>-1</sup>, respectively. In the present case, the ATR-IR spectra of **1**-PEG3 in water showed a major gauche band at ~1350 cm<sup>-1</sup> together with a small *trans* band at ~1325 cm<sup>-1</sup>. Upon increasing the PEG chain length (3 → 7 → 17), the *trans* band was diminished (Fig. S9b), indicating that the preference for the gauche conformation was further enhanced. Meanwhile, the C–C/C–O backbone vibrations were reported to show bands at ~1080 and ~1140 cm<sup>-1</sup> for the gauche and *trans* conformers, respectively. Although these two bands were overlapped and not resolved, small but substantial shifts with PEG chain length were observed (Fig. S9c), being consistent with the increase of the gauche content. Therefore, the PEG chains on the cluster behave similarly to a free polymer, exhibiting a decrease of the *trans* content with PEG chain length. Thus, the clusters covered by long PEG chains with gauche-rich characters have more polar encapsulating environments than those by short PEG chains.

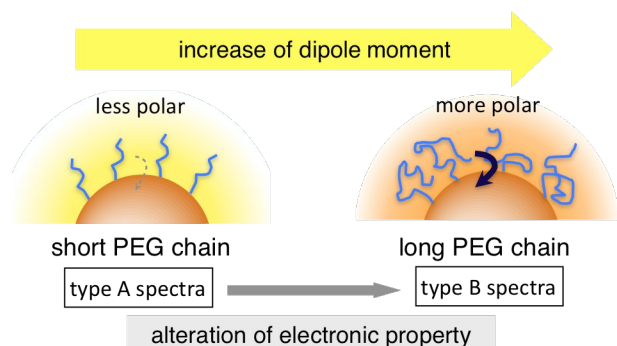


Fig. 7 Schematic illustration of the electronic perturbation effects of PEG chains on the cluster optical property.

In consequence, we now consider that the chain length dependent optical properties of **1** are correlated to the net dipole moments of the surrounding PEG layer associated with the PEG configuration. Thus, highly polar and long PEG chains notably affect the electronic states of the proximal inorganic core to give type B spectra, whereas the perturbation effects of the short PEG chains are not so significant because of their smaller dipole moments (type A) (Fig. 7). Although the possible contribution of the coordinative interaction of the distal ethylene glycol units of long PEG chains with the inorganic surface in a ‘back-biting’ manner is not completely excluded, we think that the overall polarity (dipole moment) of

the encapsulating environments primarily affect the electronic properties of the inorganic core.

## Conclusions

In this study, we have systematically investigated the absorption and photoluminescence features of a series of PEG-modified small cadmium chalcogenide clusters and have provided definitive evidence that surrounding PEG environments can uniquely electronically affect the properties of an inner inorganic core. Considering the effects of spatial separation between the PEG units and the inorganic core, sufficiently long PEG units cause notable perturbations to the electronic states of the cluster when introduced near the inorganic core. On the basis of the difference between the directly PEG-attached clusters with short and long PEG chains, we propose that the dipole moment of the proximal surface environment critically affects the electronic structures of the core altering the electronic properties of the cluster. Thus, it is implied that not only do local interactions with the inorganic surface affect the electronic properties of ligand-protected cluster compounds but also the polarity of the entire encapsulating organic shell. PEG is a ubiquitous polymer material used in various research fields because of its high hydrophilicity and chemical inertness. We have clearly demonstrated that PEG is not electronically inert in certain cases, which has implications in the design of PEG-containing materials. Considering that the electronic structure of cluster compounds are generally governed by the structure and bonding of the inorganic core moieties, it should be interesting to investigate how the dipole moment of the proximal PEG environment structurally affects the inorganic core. Structural analyses of the core units coupled with rational spectroscopic techniques are currently in progress to clarify the perturbation mechanism on the cluster electronic structures.

## Acknowledgements

This work was supported by the MEXT/JSPS Grant-in-Aids (24350063). N.F thanks Asahi Glass Foundation for scholarship. The authors also thank Mr. Takahiro Yamanaka and Ms. Ayako Morishima of JASCO cooperation for the ATR-IR measurement.

## Notes and references

- ‡ **2** and **3** commonly showed an unidentified absorption band at ~320 nm, which appears to obscure the blue-shifted thin bands in the spectra of **2**-C2-PEG17 and **2**-C3-PEG17 (Fig. S6).
- G. Schmid, *Nanoparticles: From Theory to Application, 2nd, Completely Revised and Updated Edition*, Wiley VCH, 2011.
  - M. C. Daniel and D. Astruc, *Chem. Rev.*, 2004, **104**, 293–346.
  - D. V. Talapin, J. S. Lee, M. V. Kovalenko and E. V. Shevchenko, *Chem. Rev.*, 2010, **110**, 389–458.
  - A. M. Smith and S. Nie, *Acc. Chem. Res.*, 2010, **43**, 190–200.
  - R. Jin, *Nanoscale*, 2015, **7**, 1549–1565.

6. K. Konishi, *Struct. Bond.*, 2014, **161**, 49-86.
7. N. B. Alexander, Y. Xiaohao, H. P. Joshua, L. L. Alexandra, J. Pavol, J. L. B. Simon and S. O. Jonathan, *J. Am. Chem. Soc.*, 2014, **136**, 10645-10653.
8. H. Yang, Y. Wang and N. Zheng, *Nanoscale*, 2013, **5**, 2674-2677.
9. M. T. Frederick and E. A. Weiss, *ACS Nano*, 2010, **4**, 3195-3200.
10. Y. Liang, J. E. Thorne and B. A. Parkinson, *Langmuir*, 2012, **28**, 11072-11077.
11. M. T. Frederick, V. A. Amin, N. K. Swenson, A. Y. Ho and E. A. Weiss, *Nano Lett.*, 2013, **13**, 287-292.
12. M. T. Frederick, V. A. Amin and E. A. Weiss, *J. Phys. Chem. Lett.*, 2013, **4**, 634-640.
13. M. B. Teunis, S. Dolai and R. Sardar, *Langmuir*, 2014, **30**, 7851-7858.
14. Y. Nosaka and H. Tanaka, *J. Phys. Chem. B*, 2002, **106**, 3389-3393.
15. H. Otsuka, Y. Nagasaki and K. Kataoka, *Adv. Drug Deliv. Rev.*, 2012, **64**, 246-255.
16. A. S. Karakoti, S. Das, S. Thevuthasan and S. Seal, *Angew. Chem. Int. Ed.*, 2011, **50**, 1980-1994.
17. V. J. Jesse, L. Tatsiana, N. Z. Richard and S. G. Sanjiv, *Nanomedicine*, 2011, **6**, 715-728.
18. K. Knop, R. Hoogenboom, D. Fischer and U. S. Schubert, *Angew. Chem. Int. Ed.*, 2010, **49**, 6288-6308.
19. K. Konishi, E. Takase and N. Fukunaga, *Langmuir*, 2011, **27**, 1332-1335.
20. K. Konishi and T. Hiratani, *Angew. Chem. Int. Ed.*, 2006, **45**, 5191-5194.
21. K. N. Lawrence, S. Dolai, Y.-H. Lin, A. Dass and R. Sardar, *RSC Adv.*, 2014, **4**, 30742.
22. I. G. Dance, A. Choy and M. L. Scudder, *J. Am. Chem. Soc.*, 1984, **106**, 6285-6295.
23. W. E. Farneth, N. Herron and Y. Wang, *Chem. Mater.*, 1992, **4**, 916-922.
24. T. Løver, G. A. Bowmaker, J. M. Seakins and R. P. Cooney, *Chem. Mater.*, 1997, **9**, 967-975.
25. T. Hiratani and K. Konishi, *Angew. Chem. Int. Ed.*, 2004, **43**, 5943-5946.
26. K. Konishi and T. Hiratani, *Chem. Lett.*, 2006, **35**, 184-185.
27. A. P. Alivisatos, *J. Phys. Chem.*, 1996, **100**, 13226-13239.
28. N. Yamaguchi and M. Sato, *Polym. J.*, 2009, **41**, 588-594.
29. A. Kotera, K. Suzuki, K. Matsumura, T. Nakano, T. Oyama and U. Kambayashi, *Bull. Chem. Soc. Jpn.*, 1962, **35**, 797-801.
30. M. Bjoerling, G. Karlstroem and P. Linse, *J. Phys. Chem.*, 1991, **95**.
31. R. Begum and a. Hiroatsu Matsuura, *J. Chem. Soc., Faraday Trans.*, 1997, **93**, 3839-3848.
32. S. A. Wahab and H. Matsuura, *PCCP*, 2001, **3**, 4689-4695.
33. J. J. Shephard, P. J. Bremer and A. J. McQuillan, *J. Phys. Chem. B*, 2009, **113**, 14229-14238.
34. T. Muraoka, K. Adachi, M. Ui, S. Kawasaki, N. Sadhukhan, H. Obara, H. Tochio, M. Shirakawa and K. Kinbara, *Angew. Chem. Int. Ed.*, 2013, **52**, 2430-2434.
35. O. Engkvist and G. Karlstrom, *J. Phys. Chem. B*, 1997, **101**, 1631-1633.
36. M. W. Skoda, R. M. Jacobs, J. Willis and F. Schreiber, *Langmuir*, 2007, **23**, 970-974.